# Thermodynamic geometry of black holes in the canonical ensemble

Pankaj Chaturvedi,[1,*] Sayid Mondal,[2,†] and Gautam Sengupta[2,‡]
[1]*Yau Mathematical Sciences Center, Tsinghua University, Beijing 100084, China*
[2]*Department of Physics Indian Institute of Technology, Kanpur 208016, India*

(Received 30 April 2018; published 17 October 2018)

We investigate the phase structure and critical phenomena for four dimensional Reissner-Nordström-AdS and Kerr-AdS black holes in the canonical ensemble, both for the normal and the extended phase space employing the framework of thermodynamic geometry. The thermodynamic scalar curvatures for these black holes characterize the liquid-gas-like first order phase transition analogous to the van der Waals fluids, through the $R$-Crossing method. It is also shown that the thermodynamic scalar curvatures diverge as a function of the temperature at the second order critical point.

DOI: 10.1103/PhysRevD.98.086016

## I. INTRODUCTION

Over the last several decades, the area of black hole thermodynamics has witnessed significant developments, making it an important testing ground for candidate theories of quantum gravity [1–3]. In the absence of a complete microscopic statistical description which remains an open issue, the semiclassical thermodynamic approach has led to significant insights into the phase transitions and critical phenomena for black holes. In this context the investigation of the thermodynamics of asymptotically anti–de Sitter (AdS) black holes have assumed a central role owing to the well known AdS/CFT correspondence [4]. Unlike asymptotically flat black holes, the latter are thermodynamically stable and exhibit a rich variety of phase transitions and critical phenomena. In particular, the Hawking-Page phase transition in such asymptotically AdS black holes are related to the confinement/deconfinement transition in the boundary field theory through the AdS/CFT correspondence [5]. For these reasons the study of the phase transitions and critical phenomena of asymptotically AdS black holes has received significant attention over the last two decades (see [6–11] for comprehensive references).

Unlike conventional thermodynamic systems, the phase structure of black holes is ensemble dependent as they are locally gravitating configurations. Their entropy is nonextensive and conventional thermodynamic stability arguments are not valid. In spite of this important distinction, asymptotically AdS black holes closely resemble conventional thermodynamic systems. For example, the charged Reissner-Nordstrom-AdS (RN-AdS) black holes in a canonical ensemble (fixed charge) exhibit a first order liquid-gas-like phase transition (analogous to the van der Waals fluids) culminating in a second order critical point [7,8]. In the grand canonical ensemble (fixed electric potential), however, these black holes undergo a Hawking-Page phase transition [12] to a thermal AdS space time illustrating the ensemble dependence of their phase structure.

In the recent past investigations in this area have involved an extended thermodynamic phase (state) space through the identification of the cosmological constant $\Lambda$ as a thermodynamic pressure with a corresponding conjugate thermodynamic volume [13–17]. This led to a modification of the Smarr formula and the first law requiring the identification of the Arnowitt-Deser-Misner (ADM) mass of the black hole with the enthalpy [13]. Remarkably, this approach renders the phase structure of RN-AdS and Kerr-AdS black holes in the canonical ensemble, to be identical to that of the van der Waals fluids with an exact match for the corresponding critical exponents [18–20].

In a related development, over the last two decades a consistent geometrical framework for studying phase transitions and critical phenomena for thermodynamic systems has received considerable attention. Starting from the pioneering work of Weinhold [21] and Ruppeiner [22], an intrinsic geometrical framework to study thermodynamics and phase transitions has been systematically developed. This approach involves a Euclidean signature Riemannian geometry of thermodynamic fluctuations in the equilibrium state space of the system. Interestingly, the positive definite line interval (with the dimensions of volume), connecting two equilibrium states in this

*cpankaj1@gmail.com
†sayidphy@iitk.ac.in
‡sengupta@iitk.ac.in

geometry, may be related to the probability distribution of thermodynamic fluctuations in a Gaussian approximation. Subsequently, from standard scaling and hyperscaling arguments it could be shown that the interactions in the underlying microscopic statistical basis are encoded in the thermodynamic scalar curvature arising from this geometry. Consequently, the thermodynamic scalar curvature scales like the *correlation volume* of the system and diverges at the critical point [22] (for a direct illustration see [23,24]). Notice that although this geometrical approach is thermodynamic and involves the macroscopic description of the system, it serves as a bridge to the microscopic description through the consideration of the Gaussian fluctuations in the analysis. This renders the geometrical framework described above a convenient method for the description of the thermodynamics of black holes, where a clear idea of the microscopic structure is an open issue. In this context, the sign of the thermodynamic scalar curvature $R$ provides information about the nature of the microscopic interactions as described in [25,26]. Over the last decade or so this geometrical framework has provided significant insights into the phase structure and critical phenomena for black holes [27–39]. Furthermore,the thermodynamic scalar curvature $R$ also provides a measure for the stability of the system as described in [26,40,41].

Following the above developments, one of the authors (G. S.) in the collaborations [25,42–44] established a unified geometrical framework for the characterization of subcritical, critical, and supercritical phenomena for thermodynamic systems including black holes. The geometrical characterization of the subcritical first order phase transitions involved the extension of Widom's microscopic approach to phase transitions based on the correlation length [45–47]. It was proposed that the phase coexistence at a first order phase transition implied the equality of the correlation lengths for phase coexistence at a first order phase transition. For the geometrical framework described above, this proposal translated to the crossing of the branches for the multiple valued thermodynamic scalar curvature as a function of its arguments. This was referred to as the *R-Crossing Method* and described the equality of the thermodynamic scalar curvature at a first order phase transition, and the results for disparate fluid systems exhibited a remarkable correspondence with experimental data [43,48–52]. This characterization has also been demonstrated for the first order phase transition in a dyonic charged AdS black hole in a mixed canonical/grand canonical ensemble with a fixed magnetic charge and a varying electric charge of the black hole by two of the authors (P. C. and G. S.) in the collaboration [53]. Despite this progress, the characterization of the phase structure of black holes in the canonical ensemble through the framework of thermodynamic geometry has remained an unresolved issue. As outlined in [22] the form of the thermodynamic metric is crucially dependent on the choice of the correct thermodynamic potential as a function of the thermodynamic variables. This in turn is determined by the choice of the ensemble being considered.

In this article we critically examine this unresolved issue and propose a construction for the thermodynamic geometry of four dimensional RN-AdS and Kerr-AdS black holes in the canonical ensemble for both the extended and the normal phase space. The appropriate thermodynamic potential in this case is the Helmholtz free energy as a function of the corresponding relevant thermodynamic variables. The thermodynamic metric appropriate to the canonical ensemble may then be obtained as the Hessian of the corresponding thermodynamic potential with respect to its arguments. Interestingly, the thermodynamic scalar curvature arising from our proposed geometrical construction correctly characterizes the phase structure and critical phenomena for these black holes in the canonical ensemble and matches well with the results from the conventional free energy approach. This naturally serves as an important application of the unified geometrical description described earlier, for the case of black holes [25,42–44]. In particular, it is a significant additional confirmation of the *R-Crossing Method* for the characterization of first order phase transitions described in [43,53].

This article is organized as follows: In the next two sections, II and III, we briefly review the thermodynamics and phase structure of four dimensional RN-AdS and Kerr-AdS black holes, both in the normal and the extended phase space, respectively. In Sec. IV we describe the essential elements of the framework of thermodynamic geometry. In the subsequent sections, V and VI, we describe the construction of the thermodynamic geometry for RN-AdS and Kerr-AdS black holes in the canonical ensemble and the characterization of their phase structures through the thermodynamic scalar curvature. In the concluding section, VII, we present a summary of our results and future issues.

## II. THERMODYNAMICS OF FOUR DIMENSIONAL RN-AdS BLACK HOLES

In this section, we briefly review some of the basic thermodynamic properties of four dimensional RN-AdS (charged) black holes, both in the normal and the extended thermodynamic phase space. The metric for the RN-AdS black hole is described as follows:

$$ds^2 = -f dt^2 + f^{-1} dr^2 + r^2 d\Omega_2^2. \tag{2.1}$$

Here, the lapse function $f(r)$ in the above metric is given as

$$f = 1 - \frac{2M}{r} + \frac{Q^2}{r^2} + \frac{r^2}{l^2}, \tag{2.2}$$

where the AdS length scale $l$ is related to the cosmological constant $\Lambda$ as $l = -\sqrt{\frac{6}{\Lambda}}$. The larger root of the equation

$f(r) = 0$ determines the black hole horizon at $r = r_+$. The field strength for the $U(1)$ Maxwell gauge field $A$ for the charged black hole is given as

$$F = dA, \qquad A = -\frac{Q}{r}dt, \qquad \Phi = \frac{Q}{r}. \tag{2.3}$$

The parameters $M$ and $Q$ are the ADM mass and the electric charge of the black hole, respectively, and $\Phi$ is the electric potential between the horizon and the asymptotic infinity. The Hawking temperature of the black hole is described as

$$T = \frac{1}{4\pi}f'(r) = \frac{1}{4\pi r}\left(1 + \frac{3r^2}{l^2} - \frac{Q^2}{r^2}\right). \tag{2.4}$$

.

### A. Normal phase space

For the normal phase space, the cosmological constant $\Lambda$ is held fixed, and, hence, the AdS length scale may be set to unity ($l = 1$). The Helmholtz free energy $F$ and the temperature $T$ in the canonical ensemble may be described as in [7,8]

$$F = M - TS = \frac{1}{12}\left(\frac{9Q^2}{r} + 3r - r^3\right), \tag{2.5}$$

and

$$T = \frac{1}{4\pi r}\left(1 + 3r^2 - \frac{Q^2}{r^2}\right). \tag{2.6}$$

The behavior of the free energy $F$ with the temperature $T$ is illustrated in Fig. 1 as described in [7,8]. The free energy curves for different charges exhibit a *characteristic swallowtail* structure indicating a first order small-black-hole/large-black-hole (SBH/LBH) phase transition for $Q < Q_c$, where $Q_c$ is the value of the charge at the critical point. This is analogous to the liquid-gas phase transition for the van der Waals fluids. It may be observed from Fig. 1 that the blue curve ($Q = 0.10$) and the green curve ($Q = 0.13$) correspond to $Q < Q_c$. These describe three distinct branches that constitute the *swallowtail* structure in the phase diagram. The red curve in Fig. 1 corresponds to the value of the critical charge $Q = Q_c = 0.17$, which indicates a second order phase transition at the critical point with the corresponding critical temperature $T_c = 0.257$.

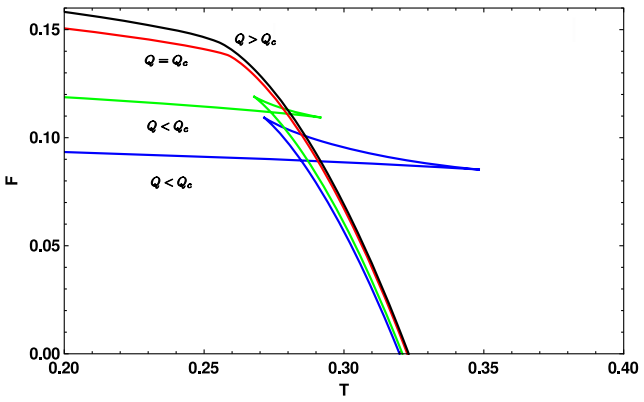


FIG. 1. Free energy: RN-AdS black holes in the normal phase space. $F$ is plotted against $T$ for different values of $Q$. Characteristic swallowtail behavior is obtained for $Q < Q_c = 0.17$, corresponding to SBH/LBH first order phase transition. At $Q = Q_c$, first order transition culminates in a second order critical point. The corresponding values of the charge $Q$ for the curves are as follows: $Q = 0.150$ (blue), $Q = 0.130$ (green), $Q_c = 0.170$ (red), and $Q = 0.175$ (black).

### B. Extended phase space

In the extended phase space, the cosmological constant $\Lambda$ is identified as the thermodynamic pressure $P$, and its variation is included in the first law of thermodynamics [13–16]. Thus, we have

$$P = -\frac{1}{8\pi}\Lambda = \frac{3}{8\pi}\frac{1}{l^2}. \tag{2.7}$$

The conjugate variable to the pressure is the thermodynamic volume $V = (\frac{\partial M}{\partial P})_{S,Q}$, which for the four dimensional RN-AdS black hole may be given as

$$V = \frac{4}{3}\pi r^3, \tag{2.8}$$

where $r$ is the radius of the horizon. In the extended phase space, the mass $M$ of the black hole is identified with the enthalpy rather than the internal energy [13], and may be expressed as

$$M = \frac{3Q^2 + 3r^2 + 8P\pi r^4}{6r}. \tag{2.9}$$

The Helmholtz free energy $F$ and the temperature $T$ for the RN-AdS black hole in the canonical ensemble may then be expressed as [18]

$$F = \frac{1}{4}\left(r - \frac{8\pi}{3}Pr^3 + \frac{3Q^2}{r}\right),$$
$$T = \frac{-Q^2 + r^2 + 8P\pi r^4}{4\pi r^3}. \tag{2.10}$$

The behavior of the free energy $F$ with the temperature $T$ for different values of the pressure $P$ and fixed values of the charge $Q$ are shown in Fig. 2 [18]. As described earlier these curves exhibit a branched *swallowtail* structure characterizing first order SBH/LBH phase transition analogous to the liquid-gas phase transition for van der Waals fluids, depicted by the blue ($P = 0.060$, $Q = 0.22$) and the green ($P = 0.065$, $Q = 0.22$) curves. It is observed that the (red curve) for the pressure $P = P_c = 0.068$, where $P_c$ is the value of the pressure at the critical point and for a fixed charge $Q = 0.220$, culminates in a second order critical point with the corresponding critical temperature as $T_c = 0.196$.

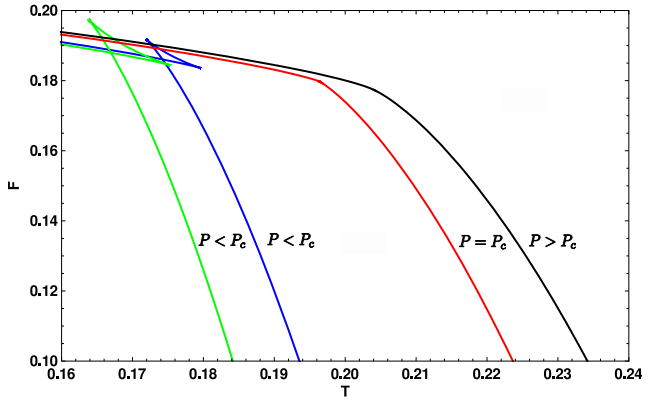


FIG. 2. Free energy: RN-AdS black hole in the extended phase space. $F$ is plotted against $T$ for a fixed $Q = 0.22$ and different pressures $P$. Characteristic swallowtail behavior is obtained below critical pressure $P < P_c = 0.068$, indicating SBH/LBH first order phase transition. The corresponding values of the pressure $P$ are as follows: $P = 0.060$ (blue), $P = 0.065$ (green), $P_c = 0.068$ (red), and $P = 0.075$ (black).

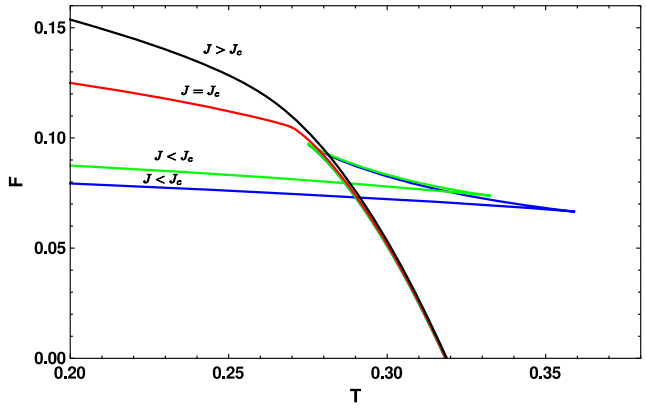


FIG. 3. Free energy: Kerr-AdS black holes in the normal phase space. $F$ is plotted against $T$ for different values of angular momentum $J$. Characteristic swallowtail behavior is obtained for $J < J_c = 0.236$, corresponding to SBH/LBH first order phase transition. The corresponding values of the angular momentum $J$ are as follows: $J = 0.01$ (blue), $J = 0.005$ (green), $J_c = 0.0236$ (red), and $J = 0.05$ (black).

## III. THERMODYNAMICS OF FOUR DIMENSIONAL KERR-AdS BLACK HOLES

In this section, we briefly review the basic thermodynamic properties of four dimensional Kerr-AdS black holes and discuss their phase structures in the canonical ensemble, for both the normal and the extended phase space. The Kerr-AdS metric in the Boyer-Lindquist coordinates is given as [54]

$$ds^2 = -\frac{\Delta}{\rho^2}\left[dt - \frac{a\sin^2\theta}{\Xi}d\phi\right]^2 + \frac{\rho^2}{\Delta}dr^2 + \frac{\rho^2}{\Delta_\theta}d\theta^2 + \frac{\Delta_\theta \sin^2\theta}{\rho^2}\left[a\,dt - \frac{(r^2+a^2)}{\Xi}d\phi\right]^2, \tag{3.1}$$

where

$$\rho^2 = r^2 + a^2\cos^2\theta, \qquad \Xi = 1 - \frac{a^2}{l^2},$$
$$\Delta = (r^2+a^2)\left(1+\frac{r^2}{l^2}\right) - 2mr, \qquad \Delta_\theta = 1 - \frac{a^2}{l^2}\cos^2\theta. \tag{3.2}$$

The corresponding thermodynamic parameters for this black hole are as follows:

$$M = \frac{m}{\Xi^2} = \frac{l^2(a^2+r^2)(l^2+r^2)}{2(a^2-l^2)^2 r}, \qquad J = \frac{ma}{\Xi^2},$$
$$\Omega_H = \frac{a\Xi}{(r^2+a^2)}, \qquad S = \frac{\pi(r^2+a^2)}{\Xi},$$
$$T = \frac{1}{2\pi}\left[r\left(\frac{r^2}{l^2}+1\right)\left(\frac{1}{a^2+r^2}+\frac{1}{2r}\right) - \frac{1}{r}\right]. \tag{3.3}$$

### A. Normal phase space

In the normal phase space the Helmholtz free energy $F$ and the Hawking temperature $T$ of the Kerr-AdS black holes in the canonical ensemble are as given below [9] (where once again the AdS length scale $l$ has been set to unity $l = 1$):

$$F = \frac{r}{4\Xi^2}[3a^2 + r^2 - (r^2-a^2)^2 + 3a^2r^4 + a^4r^2],$$
$$T = \frac{1}{2\pi}\left[r(r^2+1)\left(\frac{1}{a^2+r^2}+\frac{1}{2r}\right) - \frac{1}{r}\right]. \tag{3.4}$$

The behavior of the Helmholtz free energy $F$ with the temperature $T$ for different values of the angular momentum $J$ is shown in the Fig. 3 [9]. As earlier, these curves exhibit branched *swallowtail* structure characterizing a first order SBH/LBH phase transition for $J < J_c = 0.0236$, where $J_c$ is the value of the angular momentum at the critical point. These are illustrated by the blue ($J = 0.01$) and the green ($J = 0.005$) curves in Fig. 3. The red curve in Fig. 3 corresponds to the value of the critical angular momentum $J = J_c = 0.0236$, which indicates a second order phase transition at the critical point with the corresponding critical temperature as $T_c = 0.270$.

### B. Extended phase space

In the extended phase space, the corresponding free energy $F$ and the temperature $T$ in the canonical ensemble are as follows [55]:

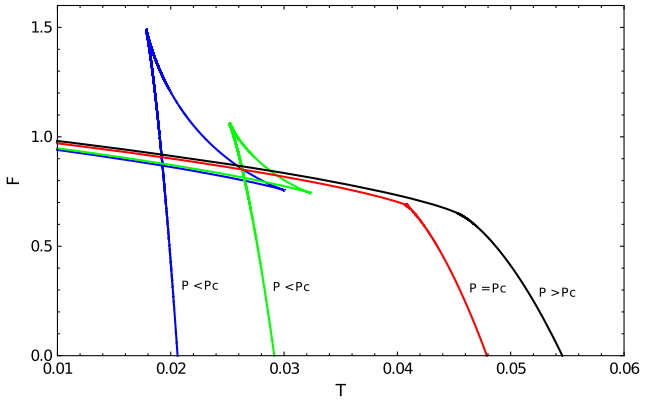


FIG. 4. Free energy: Kerr-AdS black hole in the extended phase space. $F$ is plotted for fixed $J = 1$. Characteristic swallowtail behavior is obtained for $P < P_c = 0.236$, corresponding to SBH/LBH first order phase transition. The corresponding values of the pressure $P$ are as follows: $P = 0.0005$ (blue), $P = 0.01$ (green), $P_c = 0.027$ (red), and $P = 0.0035$ (black).

$$F = \frac{r}{4\Xi^2}\left[3a^2 + r^2 - \frac{8}{3}\pi P(r^2 - a^2)^2 + \left(\frac{8}{3}\pi P\right)^2(3a^2r^4 + a^4r^2)\right],$$
$$T = \frac{1}{2\pi}\left[r\left(\frac{8\pi P r^2}{3} + 1\right)\left(\frac{1}{a^2 + r^2} + \frac{1}{2r}\right) - \frac{1}{r}\right]. \quad (3.5)$$

The behavior of the free energy $F$ with the temperature $T$ for different values of the pressure $P$ and a fixed angular momentum $J$ is depicted in Fig. 4 [54]. The free energy $F$ curves depicted by blue $(P = 0.0005, J = 1)$ and the green $(P = 0.01, J = 1)$ in Fig. 4, as earlier, illustrates the *characteristic swallowtail* structure indicating a first order phase transition for $P < P_c = 0.027$, between SBH/LBH phases analogous to the liquid-gas phase transition for van der Waals fluids. The red curve in Fig. 4 corresponds to the value of the critical pressure $P = P_c = 0.027$, which indicates the second order phase transition at the critical point with the corresponding critical temperature $T_c = 0.040$.

## IV. THERMODYNAMIC GEOMETRY IN THE CANONICAL ENSEMBLE

In this section, we briefly summarize some essential elements of the framework of thermodynamic geometry and its application to the study of thermodynamics and phase structure of black holes. The intrinsic geometrical description of equilibrium thermodynamics was first introduced by Weinhold [21] in the energy representation. Subsequently, Ruppenier[22], using the entropy representation and the elements of thermodynamic fluctuation theory, proposed a Riemannian metric (with Euclidean signature) given by the Hessian of the specific entropy $(s = S/V)$ with respect to the extensive variables $x^\mu$ as,

$$g_{\mu\nu} = -\frac{\partial^2 s}{\partial x^\mu \partial x^\nu}. \quad (4.1)$$

As mentioned earlier in the introduction, the probability distribution of thermodynamic fluctuations between two equilibrium states in the thermodynamic state space could then be related to the invariant line element for this metric in a Gaussian approximation. The thermodynamic scalar curvature $R$ for this geometry encoded the interactions in the underlying microscopic statistical system and was zero for a noninteracting system like the ideal gas. Through standard scaling and hyperscaling arguments it could be shown that the thermodynamic scalar curvature $R$ scaled as the *correlation volume* of the system

$$R \sim \xi^d, \quad (4.2)$$

where $\xi$ and $d$ are correlation length and the physical dimensionality of the system, respectively.

From the invariance of the line element under general coordinate transformations, it could be established that any Masieu function obtained through Legendre transformations could serve as a thermodynamic potential for the corresponding thermodynamic metric [22]. At the critical point, the correlation length is infinite leading to the divergence of the thermodynamic scalar curvature. It could be further shown in [23–25,42] that the thermodynamic scalar curvature $R$ was a multiple valued function of its arguments at a first order phase transition, which could be characterized by the crossing of the branches corresponding to the coexisting phases. This was termed as the *R-Crossing Method* and provided an alternative geometrical characterization to the usual free energy based condition for first order phase transitions and phase coexistence. Moreover the locus of the maxima of $R$ beyond the critical point provided a direct theoretical scheme to compute the Widom line in the supercritical region leading to a complete unified geometrical characterization of subcritical, critical, and supercritical phenomena. The *R-Crossing Method* was successfully implemented to describe the first order phase transitions for dyonic charged black holes in mixed canonical/grand canonical ensembles [53]. In the next section, we apply this geometrical characterization to study the liquid-gas-like phase behavior of RN-AdS and Kerr-AdS black holes in the canonical ensemble, both in the normal and the extended phase space described earlier.

## V. THERMODYNAMIC GEOMETRY OF RN-AdS BLACK HOLES

In this section, we construct the thermodynamic geometry of four dimensional RN-AdS black holes in the canonical ensemble, for both normal and extended phase

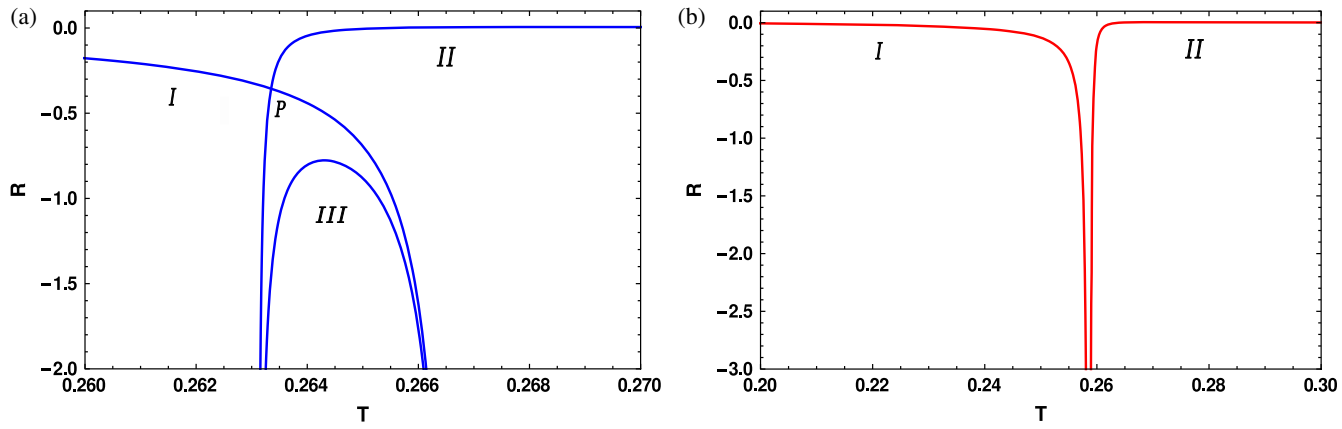


FIG. 5. Thermodynamic scalar curvatures $R$ of the RN-AdS black hole in the normal phase space for different values of $Q$: Figure (a) is plotted for $Q = 0.155$, which exhibits first order phase transition between SBH/LBH. Figure (b) is plotted at the critical charge $Q = Q_c = 0.17$, which illustrates the divergence of $R$ for the second order critical point.

space. To this end, we use the Helmholtz free energy $F$ as the thermodynamic potential to obtain the thermodynamic metric which may be expressed as [22][1]

$$g_{\mu\nu} = \frac{1}{T}\frac{\partial^2 F}{\partial x^\mu \partial x^\nu}. \tag{5.1}$$

Note that in the canonical ensemble, the charge $Q$ is held fixed, and, hence, appropriate derivatives with respect to the arguments of the Helmholtz free energy $F$ must be considered.[2] In this case these are the electric potential $\phi$ and the temperature $T$. The scalar curvature $R$ computed from this thermodynamic metric may then be examined as a function of the relevant thermodynamic variable to characterize the first order phase transition through the *R-Crossing Method* described earlier.

### A. Normal phase space

In the normal phase space, the thermodynamic scalar curvature $R$ is obtained from the metric defined by Eq. (5.1) with the extensive variables $x^\mu = (T, \phi)$, where $T$ and $\phi$ are the temperature and the electric potential, respectively. The thermodynamic scalar curvature $R$ may then be obtained from this metric as $R = N/D$, where

$$\begin{aligned} N &= 2[36Q^6 - 3Q^4r^2(21 + 32r^2) + Q^2r^4(19 + 64r^2 + 4r^4) \\ &\quad - r^6(-4 + r^2 + r^4 + 8r^6)], \\ D &= 3(-Q^2 + r^2 + r^4)(3Q^2r - r^3 + r^5)^2. \end{aligned} \tag{5.2}$$

The behavior of the thermodynamic scalar curvature $R$ with the temperature $T$ is plotted in the Fig. 5 parametrically with the radius of the horizon $r$ as a parameter. It is observed that the thermodynamic scalar curvature $R$ is a multiple valued function of the thermodynamic variables in the neighborhood of the first order phase transition similar to the free energy $F$ as shown in Fig. 1. As mentioned earlier, a first order phase transition is characterized through the *R-crossing Method* in [43,48–51] through the intersection of the branches of $R$ representing the coexisting phases. This may be understood from Fig. 5(a) for the value of the charge $Q$ less than the critical charge $Q_c$ ($Q < Q_c = 0.17$). The branches of the thermodynamic scalar curvature $R$ marked $I$ and $II$ in Fig. 5(a) describe the coexisting SBH/LBH phases at the first order phase transition, respectively. The intersection point $P$ of these two branches of $R$ in Fig. 5(b), where they cross, characterizes the first order phase transition at which these two phases coexist. The branches, collectively denoted as $III$, on the other hand, correspond to the metastable and unstable phases which are unphysical.

Comparing with the free energy plot in Fig. 1, we observe that the branches $I$ and $II$ correspond to the two arms of the swallowtail structure for the blue and the green curves, whereas the branches collectively denoted as $III$ correspond to the swallowtail portion of the free energy plot in Fig. 5(b).[3] The transition temperature for the first order

[1]Note that black holes have no notion of physical volume; hence, it is conventional to use the normal thermodynamic potential instead of the specific one in the definition of the thermodynamic metric.

[2]See also Ref. [44] for an alternate approach in the case of the extended phase space.

[3]Note, however, that in contrast to the free energy approach which is macroscopic, the framework of thermodynamic geometry constitutes a microscopic approach to phase transitions due to its connection with the thermodynamic fluctuation theory and the correlation volume. So, the correspondence between Fig. 5 and Fig. 1, described here is only approximate and not exact. We emphasize here that the geometrical approach described here is more accurate as it is directly connected to the underlying microscopic structure.

phase transition is then the temperature corresponding to the intersection point $P$ in Fig. 5.

For $Q = Q_c$ the thermodynamic scalar curvature $R$ diverges, characterizing a critical point of second order phase transition as shown in Fig. 5(b) with the corresponding critical temperature as $T_c = 0.257$. This approximately corresponds to the kink in the red curve for the free energy plot described in Fig. 1. Note once again that the critical temperatures obtained from the two plots in Figs. 5(b) and 1 are distinct but comparable.

### B. Extended phase space

In the extended phase space the thermodynamic scalar curvature $R$ is obtained from the metric Eq. (5.1) with the free energy $F$ and the temperature $T$ as given by the Eq. (2.10). The variables which serve as the coordinates in this case are $x^\mu = (T, \phi)$. The thermodynamic scalar curvature $R$ may then be expressed as $R = N/D$, where

$$\begin{aligned} N &= 36Q^6 - 3Q^4r^2(21 + 256P\pi r^2) \\ &\quad + Q^2r^4(19 + 512P\pi r^2 + 256P^2\pi^2r^4) \\ &\quad - 4r^6(-1 + 2P\pi r^2 + 16P^2\pi^2r^4 + 1024P^3\pi^3r^6), \\ D &= 3\pi(-Q^2 + r^2 + 8P\pi r^4)(-3Q^2r + r^3 - 8P\pi r^5)^2. \end{aligned} \tag{5.3}$$

As in the previous case, the behavior of the thermodynamic scalar curvature $R$ with the temperature $T$ for different values of pressure $P$ and a fixed value of the charge $Q = 0.22$ are plotted in Fig. 6 parametrically with the radius of the horizon $r$ as a parameter. It is observed from Fig. 6(a) that for $P < P_c$, where $P_c$ is the critical pressure, the two different branches $I$ and $II$ of the thermodynamic scalar curvature $R$ cross each other, indicating a first order phase transition between the SBH/LBH phases. The curves denoted as $III$ once again represent unphysical phases. For the pressure $P$ equal to the critical pressure $P_c$ ($P = P_c = 0.68$), the $R$ curve in Fig. 6(b) exhibits a divergence which describes a critical point of second order phase transition with the corresponding critical temperature as $T_c = 0.196$. As earlier, this approximately corresponds to the kink in the red curve in Fig. 2 for the free energy plot. Note that once more the critical temperatures obtained from Figs. 6(b) and 2 are distinct but comparable.

## VI. THERMODYNAMIC GEOMETRY OF KERR-AdS BLACK HOLES

In this section,we construct the thermodynamic geometry for the four dimensional Kerr-AdS black holes in the canonical ensemble for both the normal and the extended phase space. As earlier, we utilize the Helmholtz free energy $F$ to compute the thermodynamic scalar curvature $R$ from the metric Eq. (5.1). In the canonical ensemble the angular momentum $J$ is held fixed, so the appropriate thermodynamic variables are the temperature $T$ and the angular velocity $\Omega$ for the thermodynamic state space.

### A. Normal phase space

In the normal phase space, the thermodynamic scalar curvature $R$ for four dimensional Kerr-AdS black holes is obtained from the metric defined by Eq. (5.1), with the free energy $F$ and the temperature $T$ as given by Eq. (3.4). The thermodynamic variables in this case are $x^\mu = (T, \Omega)$. The corresponding thermodynamic scalar curvature $R$ may be expressed as $R = XN/D$, where

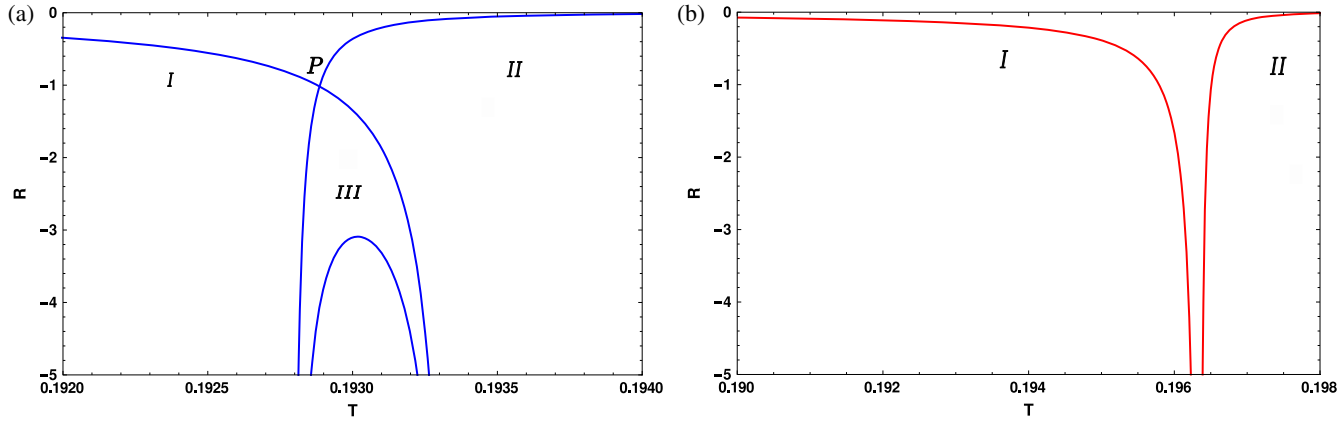


FIG. 6. Thermodynamic scalar curvature $R$ of the RN-AdS black hole in the extended phase space for fixed values of $P$ and $Q$: Figure (a) is plotted for $P = 0.065$ and $Q = 0.22$, which exhibits a first order phase transition between SBH/LBH. Figure (b) is plotted for $P = 0.068$ and $Q = 0.22$, which illustrates the divergence of $R$ for the second order critical point.

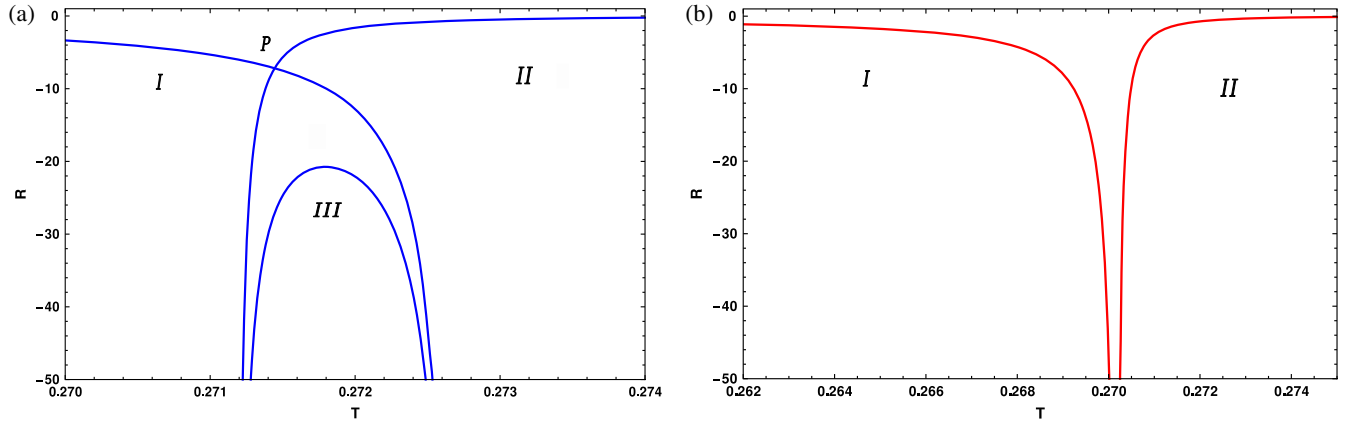


FIG. 7. Thermodynamic scalar curvatures of the Kerr-AdS black hole in the normal phase space for fixed values of $J$: Figure (a) is plotted for $J = 0.022$, which exhibits a first order phase transition between SBH/LBH. Figure (b) is plotted for the critical angular momentum $J = J_c = 0.0236$, which illustrates the divergence of $R$ for the second order critical point.

$$
\begin{aligned}
&N = A + B + C, \qquad X = 6\pi^{\frac{3}{2}}\left(\frac{S}{\pi + S}\right)^{\frac{1}{2}},\\
&A = 3(\pi - 2S)S^8(\pi + S)^7 + 12J^2\pi^3S^6(\pi + S)^5(28\pi^2 + 44\pi S + 21S^2),\\
&B = 16J^4\pi^6S^4(\pi + S)^3(66\pi^3 + 8\pi^2S - 189\pi S^2 - 126S^3) + 256J^8\pi^{13}(3\pi^3 - 21\pi^2S - 70\pi S^2 - 48S^3),\\
&C = 64J^6\pi^9S^2(\pi + S)(36\pi^4 + 44\pi^3 - 23\pi^2S^2 + 12\pi S^3 + 48S^4),\\
&D = (4J^2\pi^3 + S^2(\pi + S))^{\frac{1}{2}}[(\pi - 3S)S^4(\pi + S)^3 - 24J^2\pi^3S^2(\pi + S)^2(\pi + 2S) - 16J^4\pi^7(3\pi + 4S)]^2. \qquad (6.1)
\end{aligned}
$$

The behavior of the thermodynamic scalar curvature $R$ with the temperature $T$ for different values of the angular momentum $J$ are plotted in Fig. 7 parametrically with the entropy $S$ as a parameter for computational convenience. In Fig. 7(a) the thermodynamic scalar curvature $R$ is plotted against the temperature $T$ for the angular momentum $J$, which is less than the critical angular momentum $J = 0.022 < J_c$. As earlier, this curve once again characterizes a first order phase transition at the intersection of the two branches denoted as $I$ and $II$ describing the coexisting SBH/LBH phases. Figure 7(b) is plotted for the critical value of the angular momentum $J = J_c = 0.0236$, where the thermodynamic scalar curvature diverges, indicating a critical point of second order phase transition with the corresponding critical temperature as $T = T_c = 0.270$.

### B. Extended phase space

In the extended phase space, the thermodynamic scalar curvature $R$ for the four dimensional Kerr-AdS black holes is obtained as earlier from the metric Eq. (5.1) with the free energy $F$ and the temperature $T$ as given by Eq. (3.5). The thermodynamic variables in this case are $x^\mu = (T, \Omega)$, where the pressure $P$ is held fixed. The thermodynamic scalar curvature $R$ may then be expressed as $R = XN/D$, where

$$
\begin{aligned}
&N = A + B + C, \qquad X = -6\left(S\pi\left(\frac{3}{P} + 8S\right)\right)^{\frac{1}{2}},\\
&A = S^8(3 + 8PS)^7(-3 + 16PS) - 144J^2\pi^2S^6(3 + 8PS)^5(21 + 8PS(11 + 14PS)),\\
&B = 864J^4\pi^4S^4(3 + 8PS)^3[-99 + 32PS(-1 + 7PS(9 + 16PS))] + 62208J^8\pi^8(-27 + 8PS(63 + 16PS(35 + 64PS))),\\
&C = -6912J^6\pi^6S^2(3 + 8PS)243 + 8PS[99 + 2PS(-69 + 32PS(3 + 32PS))],\\
&D = (3 + 8PS)\sqrt{\frac{(12J^2\pi^2 + S^2(3 + 8PS)}{P}}(S^4(-1 + 8PS)(3 + 8PS)^3 + 24J^2\pi^2S^2(3 + 8PS)^2(3 + 16PS)\\
&\quad + 144J^4\pi^4(9 + 32PS))^2. \qquad (6.2)
\end{aligned}
$$

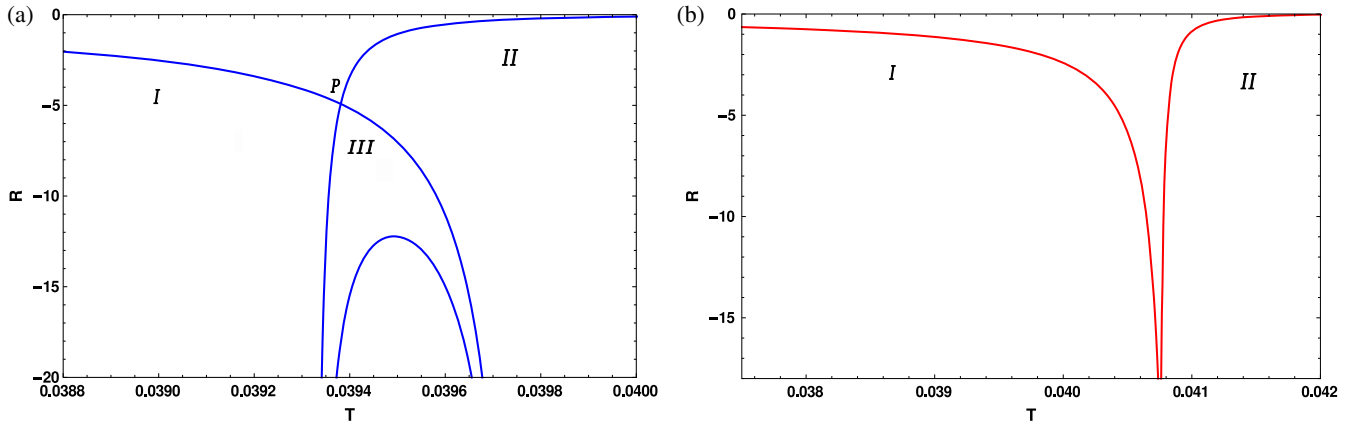


FIG. 8. Thermodynamic scalar curvatures of the Kerr-AdS black hole in the extended phase space for a fixed value of $P$ and $J$: Figure (a) is plotted for $P = 0.0025$ and $J = 1$, which exhibits a first order phase transition between SBH/LBH. Figure (b) is plotted for the critical pressure $P = P_c = 0.0027$ and $J = 1$, which illustrates the divergence of $R$ for the second order critical point.

As in the previous case, the behavior of the thermodynamic scalar curvature $R$ with the temperature $T$ for different pressures $P$ and a fixed angular momentum $J = 1$ are plotted in Fig. 8 parametrically with the entropy $S$ as a parameter. Figure 8(a), with the pressure $P$ less than the critical pressure $P = 0.0025 < P_c$, indicates a first order phase transition between the SBH/LBH phases through the intersection of the two branches denoted as $I$ and $II$ representing the coexisting phases as earlier. Figure 8(b) is plotted for the critical pressure $P = P_c = 0.0027$ and indicates a second order phase transition through the divergence of $R$ at the corresponding critical temperature $T_c = 0.040$.

## VII. SUMMARY AND DISCUSSIONS

In summary, we have investigated phase transitions and critical phenomena for four dimensional RN-AdS and Kerr-AdS black holes in the canonical ensemble, employing the framework of thermodynamic geometry both for the normal and the extended phase space. We emphasize here that the construction of the thermodynamic geometry for black holes in the canonical ensemble was an unresolved issue in this area which precluded the geometrical characterization of the corresponding phase structure for this ensemble (see also [44]). Through a careful analysis of this outstanding issue, we have determined the appropriate thermodynamic potential and the variables for the construction of the thermodynamic metric for these black holes, specific to the canonical ensemble, both for the normal and the extended thermodynamic phase space. It has been shown that the thermodynamic scalar curvature $R$ obtained from this metric clearly characterizes the phase structure for these black holes in the canonical ensemble, which conforms to the established unified geometrical characterization for phase transitions described in the literature.

For the normal phase space where the cosmological constant is held fixed, we have shown that the two branches of the thermodynamic scalar curvature $R$ describing the coexisting phases exhibit *crossing* at a first order liquid-gas-like phase transition. Interestingly, this exactly conforms to the $R$-Crossing method proposed by one of the authors earlier as part of a unified geometrical description of phase transitions. The sequence of first order subcritical phase transitions culminates in a critical point describing a second order phase transition at which the thermodynamic scalar curvature $R$ diverges as a function of the temperature. The critical temperature at the above divergence matches very well with that obtained from the conventional free energy approach.

In the extended thermodynamic phase space, the cosmological constant $\Lambda$ is identified as the thermodynamic pressure with a corresponding conjugate thermodynamic volume. This naturally leads to the modification of the first law where the variation of the thermodynamic pressure now needs to be included. As a consequence, the ADM mass of the black hole must now be identified with the enthalpy instead of the internal energy. We have shown that the thermodynamic scalar curvature also correctly characterizes the phase structure and the critical point both for the RN-AdS and the Kerr-AdS black holes in the canonical ensemble for the extended thermodynamic phase space. We emphasize here that the present article is a further confirmation of the unified geometrical approach to phase transitions and supercritical phenomena, in particular the *R-Crossing method* as applied to black holes.

It is important to further elucidate the application of this geometrical framework to study the phase structures and critical phenomena for other black holes like the Kerr-Newman-AdS black holes in the canonical ensemble, both for the normal and the extended phase space. Although our analysis in this article has been restricted to $d = 4$-dimensional RN-AdS and Kerr black holes there

are no theoretical or technical issues for its generalization to characterize standard phase transitions for higher dimensional black holes. In this context however, it should be mentioned that Born-Infeld-AdS black holes in $d = 4$ exhibit a *reentrant* phase transition for certain ranges of the black hole charge where it resembles an AdS-Schwarzschild black hole as described in [56]. Furthermore, such reentrant phase transitions have been observed in higher dimensions for $d \geq 6$, rotating Kerr-AdS black holes in [54]. A possible microscopic basis for such reentrant phase transitions for $d$-dimensional Born-Infeld-AdS and singly spinning Kerr-AdS black holes have been studied in the framework of thermodynamic geometry in higher dimensions as described in [57].

We would like to mention here that thermodynamic geometries are examples of a larger class of information geometries which involve statistical properties of systems and has been applied to diverse thermodynamic systems from fluids to black holes as described in the introduction [40,41,43,51,52,58]. In [43,51,52], this geometrical framework has been applied to the study of subcritical, critical, and supercritical phenomena, including fluids, liquids, magnetic, and optical systems. In this context the geometrical framework has led to the first theoretical construction for the Widom line in the supercritical regime for such thermodynamic systems. It would be an extremely interesting issue to explore the supercritical regime and understand the significance of the Widom line for black holes. Obtaining the critical exponents from the thermodynamic scalar curvature as described in [25] for the extended thermodynamic state space formulation would also be an important exercise in this regard. These constitute significant open issues for future investigations.

## ACKNOWLEDGMENT

We would like to thank Anurag Sahay for many useful and stimulating discussions.

[1] R. M. Wald, The thermodynamics of black holes, Living Rev. Relativity **4**, 6 (2001).
[2] D. N. Page, Hawking radiation and black hole thermodynamics, New J. Phys. **7**, 203 (2005).
[3] S. W. Hawking and D. N. Page, Thermodynamics of black holes in anti–de Sitter space, Commun. Math. Phys. **87**, 577 (1983).
[4] J. Maldacena, The large-n limit of superconformal field theories and supergravity, Int. J. Theor. Phys. **38**, 1113 (1999).
[5] E. Witten, Anti–de Sitter space, thermal phase transition, and confinement in gauge theories, Adv. Theor. Math. Phys. **2**, 505 (1998).
[6] P. C. W. Davies, Thermodynamics of black holes, Rep. Prog. Phys. **41**, 1313 (1978).
[7] A. Chamblin, R. Emparan, C. V. Johnson, and R. C. Myers, Charged AdS black holes and catastrophic holography, Phys. Rev. D **60**, 064018 (1999).
[8] A. Chamblin, R. Emparan, C. V. Johnson, and R. C. Myers, Holography, thermodynamics, and fluctuations of charged AdS black holes, Phys. Rev. D **60**, 104026 (1999).
[9] M. M. Caldarelli, G. Cognola, and D. Klemm, Thermodynamics of Kerr-Newman-AdS black holes and conformal field theories, Classical Quantum Gravity **17**, 399 (2000).
[10] C. Niu, Y. Tian, and X.-N. Wu, Critical phenomena and thermodynamic geometry of Reissner-Nordström-anti–de Sitter black holes, Phys. Rev. D **85**, 024017 (2012).
[11] Y.-D. Tsai, X. N. Wu, and Y. Yang, Phase structure of the Kerr-AdS black hole, Phys. Rev. D **85**, 044005 (2012).
[12] C. S. Peca and J. P. S. Lemos, Thermodynamics of Reissner–Nordström–anti–de Sitter black holes in the grand canonical ensemble, Phys. Rev. D **59**, 124007 (1999).
[13] D. Kastor, S. Ray, and J. Traschen, Enthalpy and the mechanics of AdS black holes, Classical Quantum Gravity **26**, 195011 (2009).
[14] B. P. Dolan, The cosmological constant and the black hole equation of state, Classical Quantum Gravity **28**, 125020 (2011).
[15] B. P. Dolan, Compressibility of rotating black holes, Phys. Rev. D **84**, 127503 (2011).
[16] M. Cvetič, G. W. Gibbons, D. Kubizňák, and C. N. Pope, Black hole enthalpy and an entropy inequality for the thermodynamic volume, Phys. Rev. D **84**, 024037 (2011).
[17] S.-W. Wei and Y.-X. Liu, Insight into the Microscopic Structure of an AdS Black Hole from a Thermodynamical Phase Transition, Phys. Rev. Lett. **115**, 111302 (2015).
[18] D. Kubizňák and R. B. Mann, $P - V$ criticality of charged AdS black holes, J. High Energy Phys. 07 (2012) 001.
[19] A. Rajagopal, D. Kubizňák, and R. B. Mann, Van der Waals black hole, Phys. Lett. B **737**, 277 (2014).
[20] S. Gunasekaran, R. B. Mann, and D. Kubiznák, Extended phase space thermodynamics for charged and rotating black holes and Born-Infeld vacuum polarization, J. High Energy Phys. 11 (2012) 110.
[21] F. Weinhold, Metric geometry of equilibrium thermodynamics, J. Chem. Phys. **63**, 2479 (1975).
[22] G. Ruppeiner, Riemannian geometry in thermodynamic fluctuation theory, Rev. Mod. Phys. **67**, 605 (1995).
[23] S. A. H. Mansoori and B. Mirza, Correspondence of phase transition points and singularities of thermodynamic geometry of black holes, Eur. Phys. J. C **74**, 2681 (2014).
[24] S. A. H. Mansoori, B. Mirza, and M. Fazel, Hessian matrix, specific heats, Nambu brackets, and thermodynamic geometry, J. High Energy Phys. 04 (2015) 115.

[25] A. Sahay, T. Sarkar, and G. Sengupta, On the thermodynamic geometry and critical phenomena of AdS black holes, J. High Energy Phys. 07 (2010) 1.
[26] B. Mirza and H. Mohammadzadeh, Ruppeiner geometry of anyon gas, Phys. Rev. E **78**, 021127 (2008).
[27] G. Gibbons, R. Kallosh, and B. Kol, Moduli, Scalar Charges, and the First Law of Black Hole Thermodynamics, Phys. Rev. Lett. **77**, 4992 (1996).
[28] S. Ferrara, G. W Gibbons, and R. Kallosh, Black holes and critical points in moduli space, Nucl. Phys. B **500**, 75 (1997).
[29] T. Sarkar, G. Sengupta, and B. N. Tiwari, On the thermodynamic geometry of BTZ black holes, J. High Energy Phys. 11 (2006) 015.
[30] T. Sarkar, G. Sengupta, and B. N. Tiwari, Thermodynamic geometry and extremal black holes in string theory, J. High Energy Phys. 10 (2008) 076.
[31] R.-G. Cai, Critical behavior in black hole thermodynamics, arXiv:gr-qc/9901026.
[32] R.-G. Cai and J.-H. Cho, Thermodynamic curvature of the BTZ black hole, Phys. Rev. D **60**, 067502 (1999).
[33] G. Ruppeiner, Black holes: Fermions at the extremal limit?, arXiv:0711.4328.
[34] J. E. Åman, I. Bengtsson, and N. Pidokrajt, Geometry of black hole thermodynamics, Gen. Relativ. Gravit. **35**, 1733 (2003).
[35] J. E. Åman, I. Bengtsson, and N. Pidokrajt, Flat information geometries in black hole thermodynamics, Gen. Relativ. Gravit. **38**, 1305 (2006).
[36] G. W. Gibbons, M. J. Perry, and C. N. Pope, The first law of thermodynamics for Kerr–anti–de Sitter black holes, Classical Quantum Gravity **22**, 1503 (2005).
[37] J. Shen, R.-G. Cai, B. Wang, and R.-K. Su, Thermodynamic geometry and critical behavior of black holes, Int. J. Mod. Phys. A **22**, 11 (2007).
[38] R. Banerjee and D. Roychowdhury, Critical phenomena in Born-Infeld AdS black holes, Phys. Rev. D **85**, 044040 (2012).
[39] R. Banerjee and D. Roychowdhury, Critical behavior of Born-Infeld AdS black holes in higher dimensions, Phys. Rev. D **85**, 104043 (2012).
[40] H. Janyszek and R. Mrugaa, Riemannian geometry and stability of ideal quantum gases, J. Phys. A **23**, 467 (1990).
[41] H. Janyszek, Riemannian geometry and stability of thermodynamical equilibrium systems, J. Phys. A **23**, 477 (1990).
[42] A. Sahay, T. Sarkar, and G. Sengupta, Thermodynamic geometry and phase transitions in Kerr-Newman-AdS black holes, J. High Energy Phys. 04 (2010) 1.
[43] G. Ruppeiner, A. Sahay, T. Sarkar, and G. Sengupta, Thermodynamic geometry, phase transitions, and the Widom line, Phys. Rev. E **86**, 052103 (2012).
[44] A. Sahay, Restricted thermodynamic fluctuations and the Ruppeiner geometry of black holes, Phys. Rev. D **95**, 064002 (2017).
[45] B. Widom, Equation of state in the neighborhood of the critical point, J. Chem. Phys. **43**, 3898 (1965).
[46] B. Widom, The critical point and scaling theory, Physica **73**, 107 (1974).
[47] H. E. Stanley, Scaling, universality, and renormalization: Three pillars of modern critical phenomena, Rev. Mod. Phys. **71**, S358 (1999).
[48] H.-O. May and P. Mausbach, Riemannian geometry study of vapor-liquid phase equilibria and supercritical behavior of the Lennard-Jones fluid, Phys. Rev. E **85**, 031201 (2012).
[49] H.-O. May, P. Mausbach, and G. Ruppeiner, Thermodynamic curvature for attractive and repulsive intermolecular forces, Phys. Rev. E **88**, 032123 (2013).
[50] G. G. Simeoni, T. Bryk, F. A. Gorelli, M. Krisch, G. Ruocco, M. Santoro, and T. Scopigno, The Widom line as the crossover between liquid-like and gas-like behaviour in supercritical fluids, Nat. Phys. **6**, 503 (2010).
[51] A. Dey, P. Roy, and T. Sarkar, Information geometry, phase transitions, and the Widom line: Magnetic and liquid systems, Physica A **392A**, 6341 (2013).
[52] A. Dey, S. Mahapatra, P. Roy, and T. Sarkar, Information geometry and quantum phase transitions in the Dicke model, Phys. Rev. E **86**, 031137 (2012).
[53] P. Chaturvedi, A. Das, and G. Sengupta, Thermodynamic geometry and phase transitions of dyonic charged AdS black holes, Eur. Phys. J. C **77**, 110 (2017).
[54] N. Altamirano, D. Kubizňák, and R. B. Mann, Reentrant phase transitions in rotating anti–de Sitter black holes, Phys. Rev. D **88**, 101502 (2013).
[55] N. Altamirano, D. Kubiznak, R. B. Mann, and Z. Sherkatghanad, Thermodynamics of rotating black holes and black rings: Phase transitions and thermodynamic volume, Galaxies **2**, 89 (2014).
[56] A. Dehyadegari and A. Sheykhi, Reentrant phase transition of Born-Infeld-AdS black holes, Phys. Rev. D **98**, 024011 (2018).
[57] M. K. Zangeneh, A. Dehyadegari, A. Sheykhi, and R. B. Mann, Microscopic origin of black hole reentrant phase transitions, Phys. Rev. D **97**, 084054 (2018).
[58] D. C. Brody and D. W. Hook, Information geometry in vapour–liquid equilibrium, J. Phys. A **42**, 023001 (2009).